

Chapter 18

Performance Evaluation of a Commercial 3D Printer that Uses Fused Filament Deposition Technology



**Secundino Ramos-Lozano, Javier Molina-Salazar, Lázaro Rico-Pérez
and David Atayde-Campos**

Abstract Since 3D printer home and industrial applications have increased in the last years, the need for a reliable tool to evaluate 3D printer capabilities has become necessary. A DOE was performed to determine the optimum parameters for dimensional accuracy and finished surface on printed pieces on a commercial 3D printer that uses fused filament deposition technique (FDM) with polylactic acid (PLA) as print material. A 3D digital model with geometric internal and external features was generated with a CAD software; this model was used to print two sets of physical samples, one set with the 3D printer adjusted according to DOE optimal settings results and the other set with the manufacturer recommended setup. Measurement system analysis bias was applied to evaluate the dimensional and geometrical performance of the 3D printer for each set. Samples were measured and compared against dimensional specifications on the drawing. No evidence of works related to the finished surface or geometrical analysis was found in the literature reviewed about 3D printed models. Finished surface was evaluated, and it was found that roughness depends mainly on the layer thickness of lateral walls of the piece, while on the upper face, the infill density has a major influence on the finished part. Most geometries and dimensions were rejected according to bias criteria, and no significant difference was found between both evaluated setups, so the printed models should be used only where dimensional accuracy is not critical. MSA bias can be used as an alternative method to make a dimensional and geometrical evaluation of printed models on 3D printers.

Keywords 3D printer · CAD · FDM · PLA

S. Ramos-Lozano (✉) · J. Molina-Salazar · L. Rico-Pérez · D. Atayde-Campos
Department of Industrial Engineering and Manufacturing, Universidad Autónoma
de Ciudad Juárez, Av. Del Charro 450 Norte. Col. Partido Romero,
Juárez, Chihuahua, Mexico
e-mail: secundino.ramos@uacj.mx

© Springer Nature Switzerland AG 2019
J. L. García Alcaraz et al. (eds.), *Best Practices in Manufacturing Processes*,
https://doi.org/10.1007/978-3-319-99190-0_18

389

18.1 Introduction

3D printing is a technology which converts 3D computer-aided design (CAD) data into a physical prototype (Dawoud et al. 2016). The beginning of the additive manufacturing dates back to 1976, with the invention of the inkjet printer. In 1984, designers modified technology and created the first 3D printer with some adaptations and improvements on the concept of the inkjet printer. Now, this print technology is able to work with different materials. Figure 18.1 shows different 3D printing techniques.

Figure 18.1a shows the first method created by Charles Hull, who introduced the first 3D printer using stereolithographic (SLA) technique; SLA is a photopolymerization process where a build tray is submerged in a basin of photosensitive liquid material. The basin depth varies based on laser strength, material, or desired tolerance. A UV laser (not lamp) solidifies one slice of the part onto the build tray. Then, the tray is submerged, and the laser solidifies the next slice of the part. The layer thickness affects the quality of the print and its tolerances. The laser travels the entire path of the part's cross section as it builds up each layer, so the speed becomes an important consideration. When the part is complete, the printer drains the resin excess, which is reusable. The operator washes the formed parts to remove resin excess and the support structures are physically removed (Stanbury 2016).

Figure 18.1b shows the laser printing technology (SLS) developed in 1986. SLS process uses a layer of powdered material carefully laid down by a leveler or roller on the build tray. Then, a laser sinters the part's cross section, and the tray goes down to repeat the process. Similar to SLA, layer thickness varies based on laser strength, material, or desired tolerance.

Figure 18.1c shows a widely used 3D printing technique called fused deposition modeling (FDM), introduced by the end of the 80s. The printer melts the filament of material in a heated nozzle and leaves it on a platform, once the printer finishes the

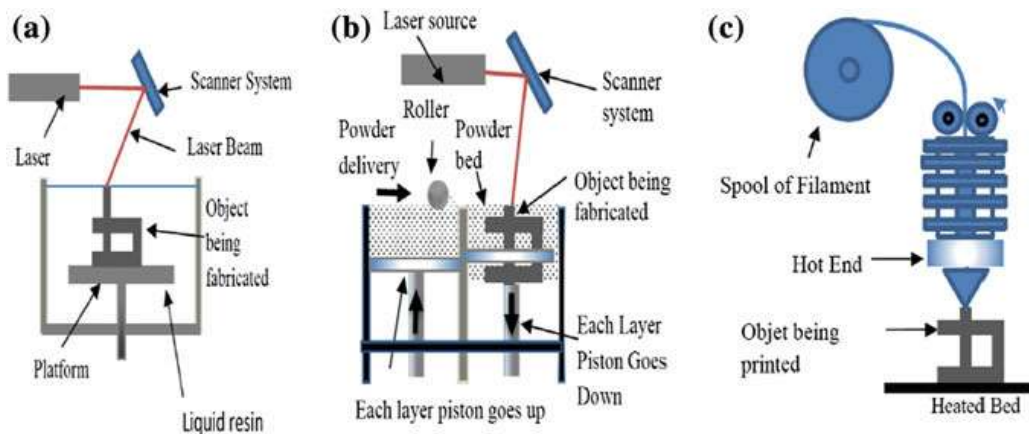


Fig. 18.1 3D printer technologies

layer, the platform lowers a layer thick on the Z axis and the next layer deposition begins. The printer may leave a secondary sacrificial material to support the construction of overhanging geometries.

The choice of printing material depends on the type of application and desired properties. Commonly applied materials include polylactic acid (PLA) as a stiff and environmentally friendly material, nylon, for soft applications, high-density polyethylene (HDPE) for the production of food compatible parts, and acrylonitrile butadiene styrene (ABS) a solution for tough parts with acceptable strength (Dawoud et al. 2016).

There are different techniques for creating layers on 3D printing, from jetting a binder into a polymeric powder, using an ultraviolet laser to harden a photosensitive polymer (stereolithographic), to using a laser to selectively melt metal or polymeric powder (laser sintering) (Campbell et al. 2011).

In the last decades, several industries developed a great variety of applications of 3D printing technology. Additive manufacturing processes make three-dimensional objects of almost any form, based on digital models through successive layers of material placed on a print platform under numerical control (Satyyanarayana and Jaya 2015) and generate less waste than traditional subtractive production methods.

Digital models are usually created using computer-aided design (CAD) software. In addition, 3D scanners automatically generate digital models from physical objects (just like 2D scanners are used to digitize photos, drawings or documents) (Rayna and Striukova 2016).

The adoption of additive manufacturing and other manufacturing technologies predicts a future in which chains value are shorter, smaller, more localized, more collaborative, and able to deliver substantial benefits of sustainability (Gebler et al. 2014). Figure 18.2 shows a generalized 3D printing process starting with the creation of a digital model and finishing with the part printed.

The accessibility of 3D printers for industrial and general public applications has grown dramatically in the past decade (Stanbury 2016), due mainly to the price

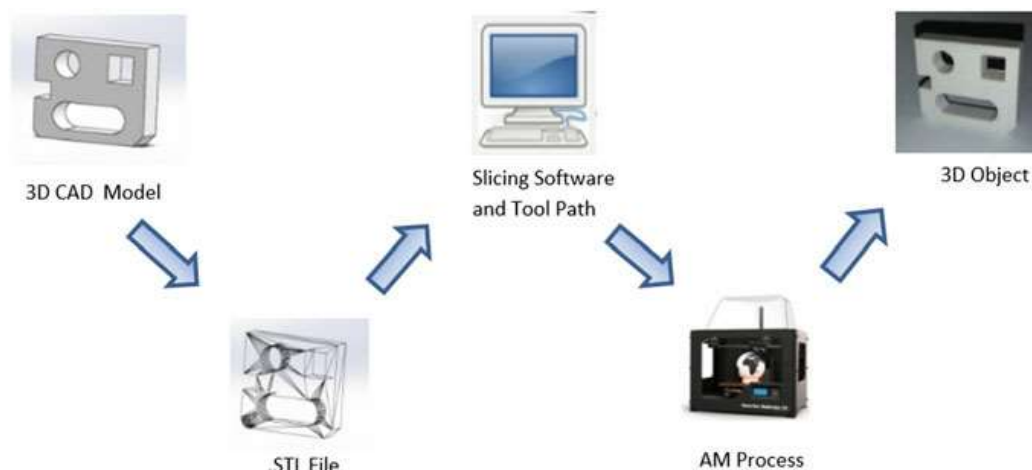


Fig. 18.2 Generalized additive manufacturing process

drop and to the vast quantity of applications found on 3D printers. Currently, this technology has a major impact on objects that could cost up to \$30,000 dollars in the traditional industry; 3D printers give almost the same quality for less than \$2000 (Evans 2012); however, the results do not allow their use in finished products, leaving their use mainly relegated to prototypes and pre-series (Cajal et al. 2013). The increase in the number of low-cost 3D printers on the market and a wide range of manufacturers makes the evaluation of the capabilities of different 3D systems paramount to the proliferation of low-cost additive manufacturing in terms of consumer confidence in this technology.

Since 3D printer home applications have increased substantially, a need to establish a tangible metric to evaluate the units' accuracy in an easier way is necessary. For the time being, we have been unable to identify a tool to evaluate the consumer worthiness of an additive manufacturing unit (Roberson et al. 2013).

Manufacturers of commercial 3D printers provide little or none information in terms of the quality of the manufactured product, such as reproducibility in extruder positioning, dimensional and geometric precision, surface texture, and crucial data for established elements (Nunez et al. 2015). Dimensional and geometric accuracy can be improved by reducing print speed but increasing the overall printing time (Galantucci et al. 2015).

This work evaluates the geometrical and dimensional performance of a commercial 3D printer (Flashforge Creator Pro) analyzing printed samples under vendor recommended specifications in order to determine the performance and accuracy of the printer using PLA material.

18.2 Materials and Methods

18.2.1 3D Printer

The Flashforge Creator Pro (FlashforgeUSA™) is a 3D printer with a dual extruder that uses fused deposition filament technology, capable of processing ABS and PLA printing material with a resolution up to 100 μm for each layer and a print space of 22.5 cm \times 14.5 cm \times 15.0 cm (4893.75 cm³).

The print material selected for the analysis is a 1.75 mm diameter PLA filament fused at 180–220 °C during the printing process. This 3D printer is compatible with .STL and .OBJ files on Windows, Mac, and Linux operating systems. The extruder moves through X–Y planes putting fused PLA material on the print bed that moves down on the Z plane allowing the extrusion to place a new layer until a physical model is formed.

SolidWorks 2016 (Dassault Systemes 2016) is the software used to generate digital model saved as .STL file (stereolithography). This type of file created by the company 3D systems is compatible with several commercial software, and it is widely used for rapid prototyping and computer-aided manufacturing.

A .STL model is transferred to a Flashforge Creator Pro printer (FlashfogeUSA 2017) that uses a software called Replicator G (Hoeken et al. 2012) which makes the slicing operation, calculates the extruder path, and generates the G code to communicate the printer commands in order to build the 3D object.

18.2.2 DOE for Printer Settings Selection

The 2^k designs (k corresponds to the number of factors or printer settings to be analyzed and 2 refers to the number of levels for each factor) are particularly useful when there are many factors to be investigated, since they provide the smallest number of runs using k factors that can be studied in a complete factorial design. Because there are only two levels of each factor, we assume that the response is approximately linear over the range of the factor levels chosen (Montgomery 2001). The levels are “low” and “high”.

Five factors could influence the dimensional performance of the Flashforge Creator Pro 3D printer. These are: Extruder temperature, the levels selected are within the range of melting temperature to print with PLA filament; infill density that refers to the material inside the contour of the piece printed; infill percentage could have a value of 0% (no material inside the printed part) to 100% where no empty space left; layer thickness is the height of each material layer stacked during the printing process; and number of shells refers to the perimeter thickness. Infill density and number of shells levels chosen give good mechanical properties, and print speed refers to the printer speed. Faster 3D print speed generally means a lower quality of the printed part and problems, as the filament tends to slip at higher speeds. Levels of layer thickness and print speed selected range result in a good quality print and a reliable printing process. Table 18.1 shows the low and high DOE levels factors and the recommended manufacturer settings.

In this study, we performed a 2^5 DOE full factorial plan in order to determine the main effects that affect the dimensional performance of the 3D printer with one replication for a total of 32 experiments. Table 18.2 shows the full factor array with all the possible combinations of the five factor levels performed in the experiment.

Table 18.1 Selected factors and its corresponding values

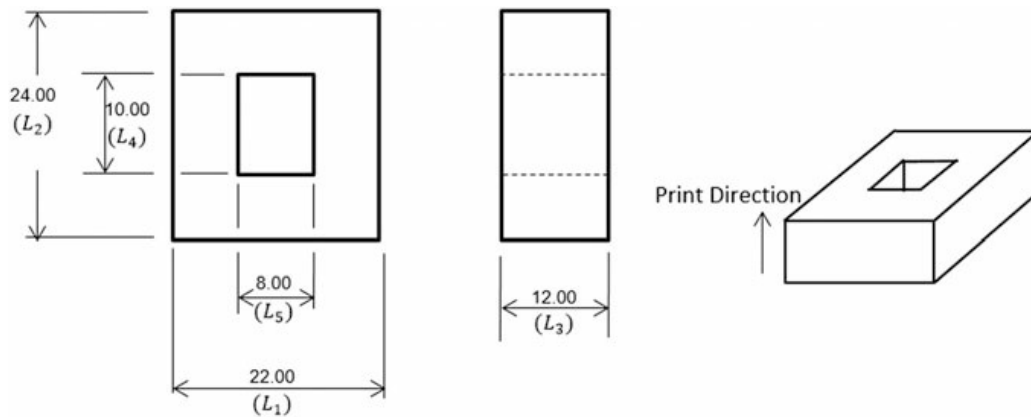
Factor	Low level (1)	High level (2)	Manufacturer recommended settings
Extruder temperature (°C)	190	220	220
Infill density (%)	20	60	10
Layer thickness (mm)	0.178	0.270	0.200
Print speed (mm/s)	40	70	80
No. of shells	1	3	1

Table 18.2 Full factorial 2^5 array

Std. order	Extrude temp. (°C)	Infill density (%)	Layer thickness (mm)	Print speed (mm/s)	Number of shells
1	190	20	0.178	40	1
2	220	20	0.178	40	1
3	190	60	0.178	40	1
4	220	60	0.178	40	1
5	190	20	0.270	40	1
6	220	20	0.270	40	1
7	190	60	0.270	40	1
8	220	60	0.270	40	1
9	190	20	0.178	70	1
10	220	20	0.178	70	1
11	190	60	0.178	70	1
12	220	60	0.178	70	1
13	190	20	0.270	70	1
14	220	20	0.270	70	1
15	190	60	0.270	70	1
16	220	60	0.270	70	1
17	190	20	0.178	40	3
18	220	20	0.178	40	3
19	190	60	0.178	40	3
20	220	60	0.178	40	3
21	190	20	0.270	40	3
22	220	20	0.270	40	3
23	190	60	0.270	40	3
24	220	60	0.270	40	3
25	190	20	0.178	70	3
26	220	20	0.178	70	3
27	190	60	0.178	70	3
28	220	60	0.178	70	3
29	190	20	0.270	70	3
30	220	20	0.270	70	3
31	190	60	0.270	70	3
32	220	60	0.270	70	3

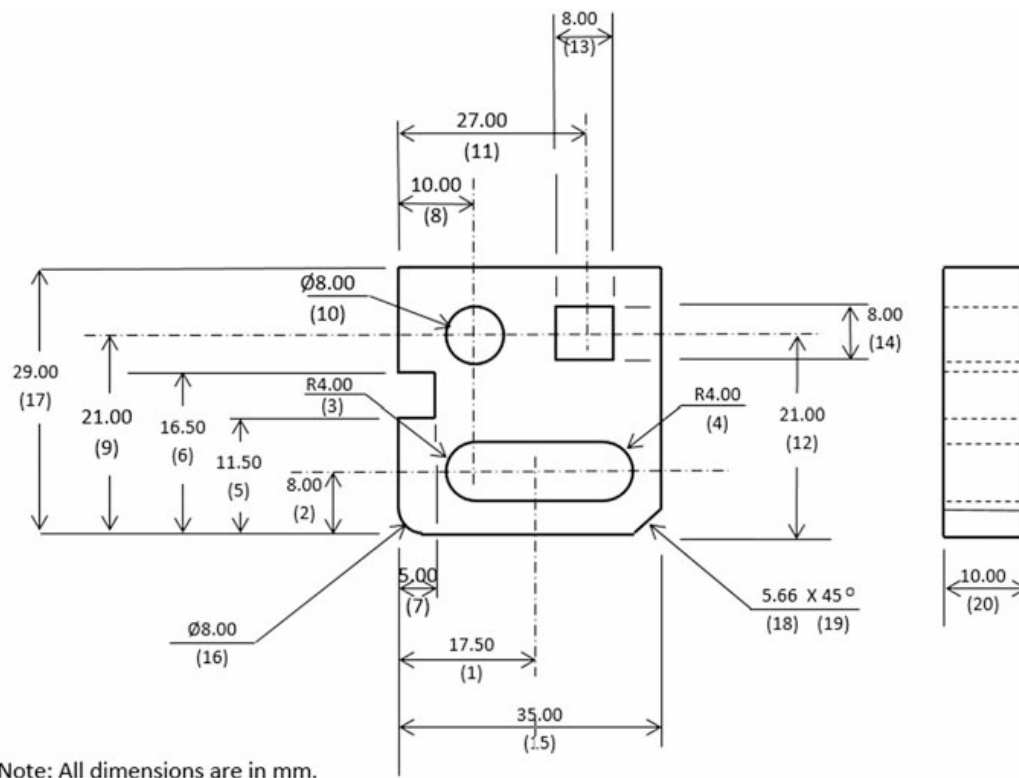
18.2.3 Model Design

Figure 18.3 shows a designed rectangular workpiece of $L_1 = 22$ mm, $L_2 = 24$ mm, $L_3 = 12$ mm, with an internal cubic feature of $L_4 = 10$ mm, $L_5 = 8$ mm, $L_3 = 12$ mm, in order to perform volume and roughness analysis. The calculated error



Note: All dimensions are in mm.

Fig. 18.3 Sample design with an internal square feature used for DOE



Note: All dimensions are in mm.

Fig. 18.4 Model drawing

is the difference between the measured and the nominal value of the workpiece volume, used as a response in order to determine the factor that influences the dimensional accuracy.

Figure 18.4 shows the sample model of 35 mm length, 29 mm width, and 10 mm thickness designed for dimensional and geometric analysis to facilitate the

dimensional measurements including labeled dimensions as radio, chamfer, and basic internal features. We adjusted the Flashforge Creator Pro 3D printer according to the DOE's factor levels to obtain the optimal printer settings in order to optimize dimensional and roughness parameters using PLA printing material.

18.2.4 Dimensional and Roughness Measurement

We measured all printed samples using a PH14-A Mitutoyo profile projector; which uses a horizontal optical system with a resolution of 0.001 mm, and a 10X projection lens. The projector uses a QM DATA 200 coordinate system alignment function to align the workpiece and the axes. We measured roughness using an SJ210 Mitutoyo SurfTest high resolution, with a measuring range of 17.5 mm on the X axis, and speed of 0.25, 0.5, 0.75 mm/s. We measured the roughness at vertical (lateral surface) and the horizontal plane (upper surface).

18.2.5 Dimensional Analysis

The measurement system analysis (MSA) workgroup manual contains an important method used to analyze the system variation called bias. The bias is a systematic error component of the measurement system that evaluates the difference between the observed measurements average and the reference value (accepted value of an artifact).

Figure 18.5 shows a graphical description of bias concept. In general, the bias or linearity error of a system is acceptable if it is not statistically significantly different from zero when compared to repeatability. Consequently, the repeatability must be acceptable when compared to the process variation in order to be useful (Automotive Industry Action Group 2010). In this work, the bias determines the location variation of the features measured to make the geometric study.

We performed the following steps in order to make this research:

1. For each reading, Eq. (18.1) calculates the difference between the measurements average and the reference value.

$$\text{bias}_i = x_i - \text{reference value} \quad (18.1)$$

2. Equation (18.2) calculates the average bias of the n readings.

$$\text{Average bias} = \bar{x} - \text{reference value} \quad (18.2)$$

3. Equation (18.3) computes the repeatability standard deviation (σ_r).

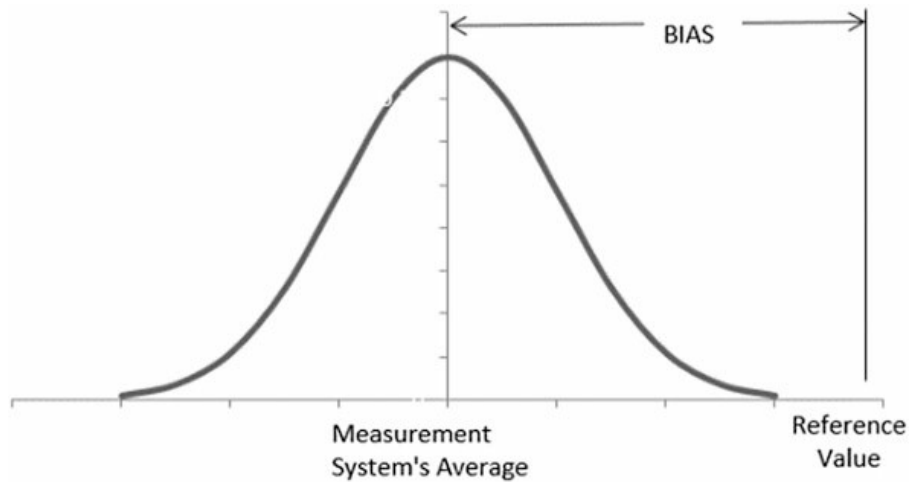


Fig. 18.5 BIAS. *Source* MSA

$$\sigma_r = \frac{\text{Max}(x_i) - \text{Min}(x_i)}{d_2^*} \quad (18.3)$$

$\text{Max}(x_i)$ is the maximum measurement reading, $\text{Min}(x_i)$ is the minimum measurement reading and d_2^* is obtained with $g = 1$ and $m = n$ of “Values Associated with the Distribution of Average Range” table located on Append C of the MSA manual.

4. Equation (18.4) determines the t statistics for the bias.

$$t_{\text{statistic}} = t_{\text{bias}} = \frac{\text{average bias}}{\sigma_r / \sqrt{n}} \quad (18.4)$$

5. Equation (18.5) gives the uncertainty for the bias σ_b .

$$\sigma_b = \sigma_r / \sqrt{n} \quad (18.5)$$

6. Equation (18.6) establishes the criteria: bias is acceptable at the α level if zero falls between $1 - \alpha$ confidence bounds based on the bias value.

$$\text{Bias} - \left[\frac{d_2 x \sigma_b}{d_2^*} (t_{v, 1-\alpha/2}) \right] \leq 0 \leq \text{Bias} + \left[\frac{d_2 x \sigma_b}{d_2^*} (t_{v, 1-\alpha/2}) \right] \quad (18.6)$$

Standard t tables use $v = n - 1$ and $t_{v, 1-\alpha/2}$ (Walpole et al. 1999).

18.2.6 Geometric Analysis

Geometric tolerances specify the maximum variation allowed on form, orientation, and location of an element workpiece. A positional geometric tolerance is the width of the diameter or a tolerance zone within some surface axis of a hole or cylinder must remain in order to meet the functional part requirements or appropriate interchangeability (Warren and Duff 1994). True position tolerance increases the permissible tolerance in all directions; the real position takes into account all the relationships that must be kept in the assembly of interchangeable parts. We performed the geometric analysis locating the center of geometric figures and computing the difference against the drawing specification. The drawing specifies geometric tolerances in accordance with functional requirements although manufacturing and inspection requirements can also influence the geometric tolerance (ISO 1101 2012). Equation (18.7) calculates the deviation from the center of the internal features on the sample respect the center specified on the drawing.

$$\oplus = 2 * \sqrt{(x_2 - x_1)^2 + (y_2 - y_1)^2} \quad (18.7)$$

The coordinates (x_1, y_1) are the values specified on the drawing and (x_2, y_2) are values measured on the profile projector.

18.2.7 Surface Analysis

The aim of this study is to find the optimal printer parameters to obtain the best quality surface by evaluating the factors selected for the dimensional performance. We used the same printed parts as in the DOE for dimensional and geometrical analysis because parts dimensions allow enough sampling surface for the roughness analysis. We used the same procedure and factor levels considered for dimensional accuracy to perform the surface analysis. Since there is a considerable roughness difference between lateral and upper surfaces, we performed the analysis in separate events.

The arithmetic mean surface roughness R_a is one of several different parameters that describe the deviation of a surface from an ideal level, and it is defined according to the international standard ISO 4287-1997 (ISO4287 1997); Eq. (18.8) defines the arithmetic mean surface roughness R_a and describes the deviation of the surface from a theoretical centerline R_{mean} . Figure 18.6 shows both R_a , and R_{mean} . Over a measurement length L_m (Stahl et al. 2011).

$$R_a = \frac{1}{L_m} * \int_0^{L_m} |y| * dx \quad (18.8)$$

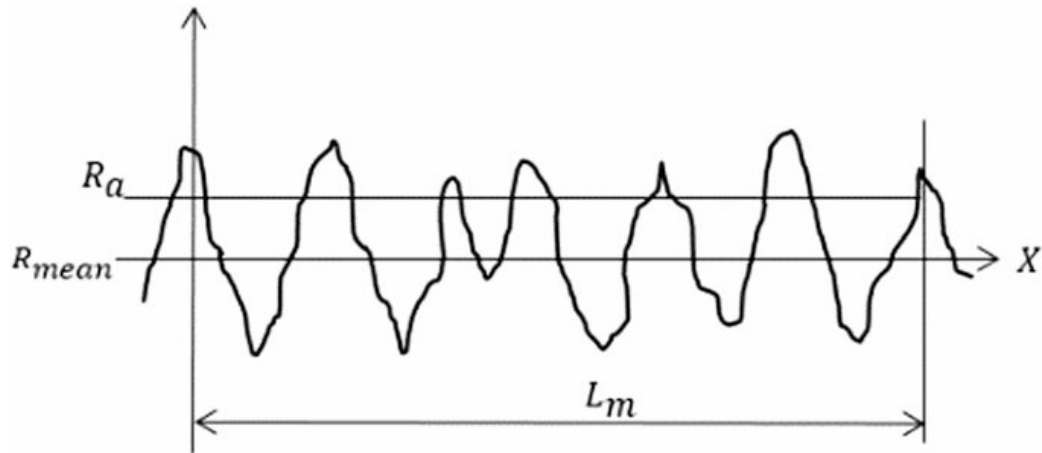


Fig. 18.6 Surface profile showing R_a and R_{mean}

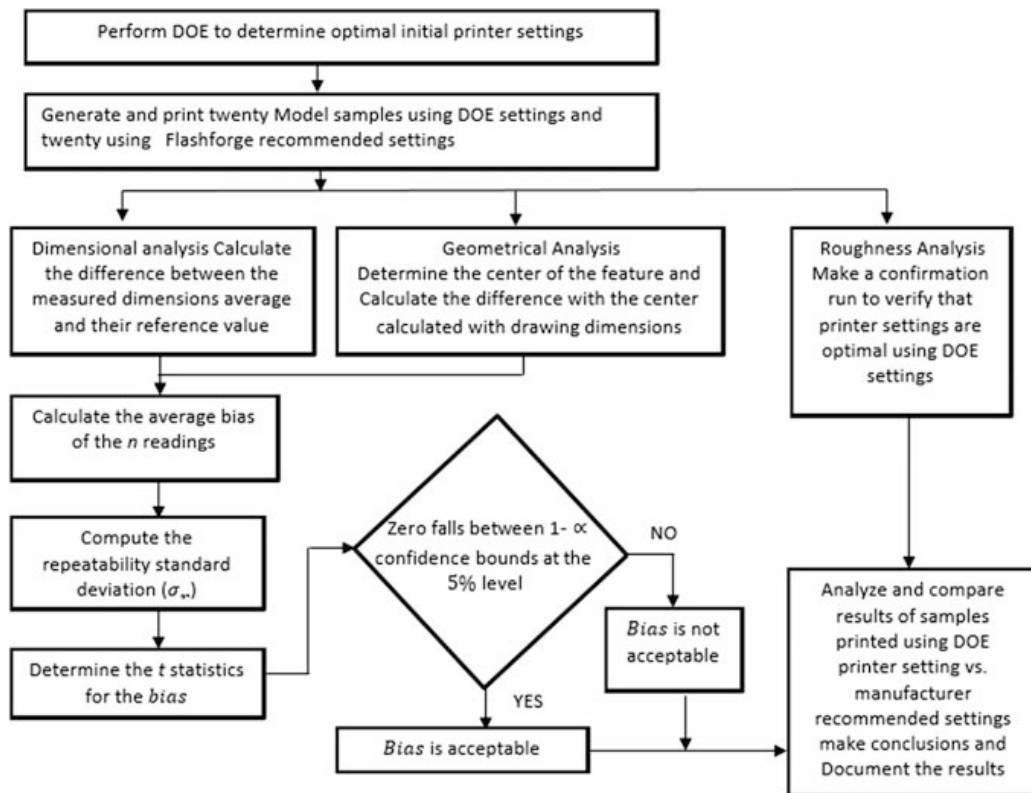


Fig. 18.7 Method diagram

We measured roughness at three locations along the lateral surface and the average of these measurements is the response to the factorial analysis, we applied the same procedure to the upper surface area.

Figure 18.7 shows all the steps taken to analyze Flashforge 3D printer dimensional and finished performance, beginning with a DOE to establish the initial 3D

printer settings that give a better dimensional and roughness performance using PLA as print material. We printed 20 samples for the analysis using DOE optimal settings and 20 samples using Flashforge recommended settings. For roughness analysis, we performed a confirmation run to verify if DOE results are better than samples printed using the manufacturer recommended setup.

MSA methodology analysis determines the dimensional and geometrical performance of the Flashforge printer with a confidence level of 95%. We labeled each dimension in the drawing with a consecutive number to make easier the comparative process and keep traceability of the dimensions. We compared the average of the 20 dimensions against drawing specification. If zero falls between confidence bounds, the deviation of the reference value (bias) is acceptable.

18.3 Results

Table 18.3 shows the measured value of length, width, and height of the printed samples. Column seven shows the calculated volume $L_1 * L_2 * L_3$ and column eight gives the volume of the internal square feature $L_4 * L_5 * L_3$. Column nine shows the measured roughness for the lateral side of the part and column ten the upper surface roughness measurement expressed in μm . These values are the response in the factorial design to define the significant factors for dimensional and roughness analysis.

18.3.1 External Volume Response Analysis

Figure 18.8 shows the Pareto chart of the effects for the external volume. We used the hypothesis testing to verify if the factors and their interactions have a significant effect on the response. Analyzing the external dimensional test, the main effect (D) and the five terms interaction (ABCDE) have a significant effect over the external dimensions and consequently, they affect the volume involved with these dimensions.

When an interaction is significant, it has priority over main individual effects to select the optimal factor levels. Since five terms interaction is significant no main terms or interactions can be eliminated, so all factors should be controlled to optimize the response. Figure 18.9 shows the results obtained from Minitab17 response optimizer to determine the optimum level of each factor. Since all factors are significant for external dimensions, the factor levels should be adjusted according to the values listed in order to get the optimal dimensional performance.

Table 18.3 Nominal and measured values

Run	L_1 (mm) (X axis)	L_2 (mm) (Y axis)	L_3 (mm) (Z axis)	L_4 (mm) (Y axis)	L_5 (mm) (X axis)	External volume (mm ³)	Internal volume (mm ³)	R_a lateral (μm)	R_a upper (μm)
Nominal	22.00	24.00	12.00	10.00	8.00	6336.00	960.00		
1	21.95	24.02	11.88	9.92	8.02	6263.60	945.15	11.436	3.663
2	21.96	24.05	11.83	9.96	8.03	6247.87	946.15	12.333	6.921
3	21.96	24.05	11.85	9.95	7.97	6258.44	939.72	12.033	4.303
4	22.05	24.08	11.88	9.84	7.97	6307.85	931.69	12.164	4.266
5	21.95	24.09	11.80	9.94	7.94	6239.55	931.30	19.607	7.703
6	22.06	24.11	11.84	9.90	8.00	6297.30	937.73	18.941	5.748
7	21.95	24.15	11.79	9.87	7.90	6249.79	919.30	19.204	7.157
8	22.08	24.16	11.78	9.70	7.72	6284.07	882.13	17.679	6.213
9	21.94	24.07	11.89	9.98	8.03	6279.06	952.86	11.945	5.843
10	22.09	24.13	11.86	10.08	8.05	6321.76	962.37	12.993	8.746
11	22.01	24.10	11.90	9.98	8.02	6312.25	952.47	11.027	4.846
12	22.17	24.17	11.83	9.97	7.90	6339.09	931.77	11.899	6.708
13	21.98	24.22	11.88	9.91	7.89	6324.38	928.90	18.110	6.977
14	22.12	24.19	11.78	9.99	8.06	6303.28	948.52	18.155	7.557
15	22.10	24.18	11.82	9.95	7.76	6316.35	912.65	17.767	7.652
16	22.23	24.26	11.81	9.84	7.85	6369.13	912.25	18.404	9.659
17	21.91	24.01	11.84	10.06	8.03	6228.54	956.46	19.201	4.979
18	21.97	24.09	11.87	9.99	8.06	6282.28	955.77	11.522	7.062
19	21.94	24.04	11.86	9.98	7.97	6255.41	943.35	14.005	4.156
20	21.97	24.04	11.81	10.06	7.99	6237.56	949.28	11.892	5.468
21	22.03	24.15	11.88	9.79	7.80	6320.45	907.18	21.158	11.443
22	22.09	24.16	11.75	9.81	7.94	6270.91	915.22	19.394	11.406
23	21.99	24.15	11.80	9.82	7.92	6266.49	917.74	19.593	9.163
24	22.07	24.11	11.74	9.67	7.69	6246.94	873.01	17.923	9.119
25	21.96	24.05	11.91	9.95	7.97	6290.12	944.48	10.911	7.601
26	22.07	24.12	11.84	9.90	7.85	6302.77	920.15	13.215	12.460
27	21.99	24.05	11.85	10.00	7.90	6266.99	936.15	12.285	6.168
28	22.10	24.11	11.84	10.03	8.05	6308.72	955.98	11.324	10.449
29	21.99	24.07	11.87	10.06	8.08	6282.78	964.85	11.270	7.532
30	22.08	24.19	11.74	9.98	8.02	6270.51	939.66	17.866	7.828
31	21.98	24.12	11.90	9.87	7.88	6308.88	925.53	18.083	10.436
32	22.14	24.08	11.80	9.94	8.00	6290.95	938.34	18.322	13.417

18.3.2 Internal Volume Response Analysis

Figure 18.10a shows the Pareto chart before we eliminated all nonsignificant effects, and Fig. 18.10b shows the model with all the nonsignificant terms removed. The selections begin with higher order interactions until it is not possible to remove

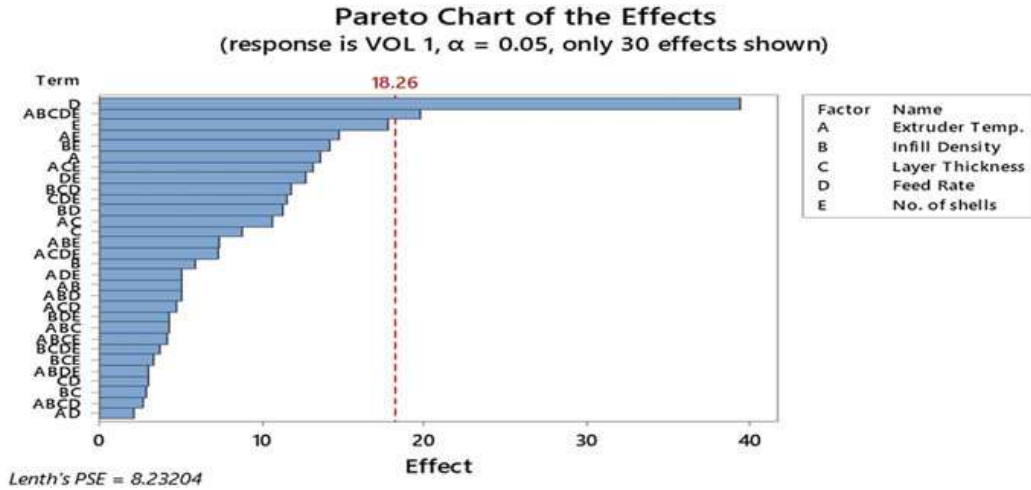


Fig. 18.8 Pareto chart of the factors effects of external volume

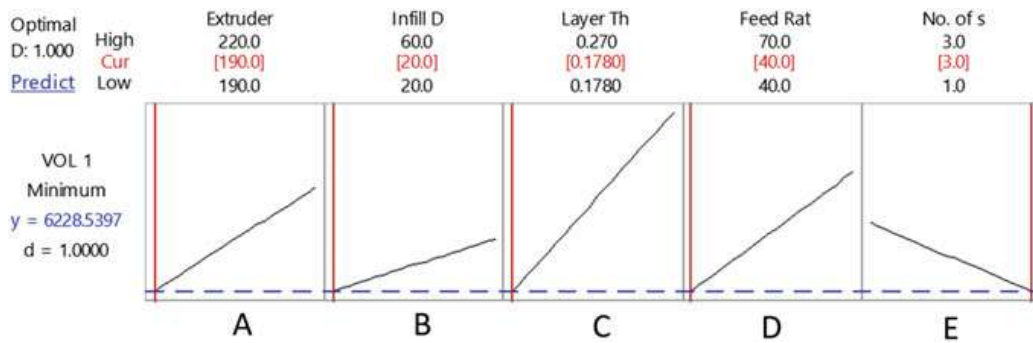


Fig. 18.9 Optimal values for external volume using optimizer Minitab tool

the terms since they are included in the significant effects. Figure 18.10b helps to determine which factors should be controlled since they have a direct impact on the response. Figure 18.11 shows the results obtained to optimize the response for internal dimensions. For the extruder temperature (A), there is almost no difference between low and high levels for this factor. Thus, this is the only nonsignificant term for the internal dimensions and it may be low or high.

18.3.3 Lateral Surface Roughness Response Analysis

Figure 18.12a shows the Pareto chart before the elimination of all nonsignificant effects for the lateral surface roughness. Figure 18.12b shows the results of the analysis using Minitab after all the nonsignificant terms have been removed for lateral surface roughness test, two main effects (C and D) and one interaction

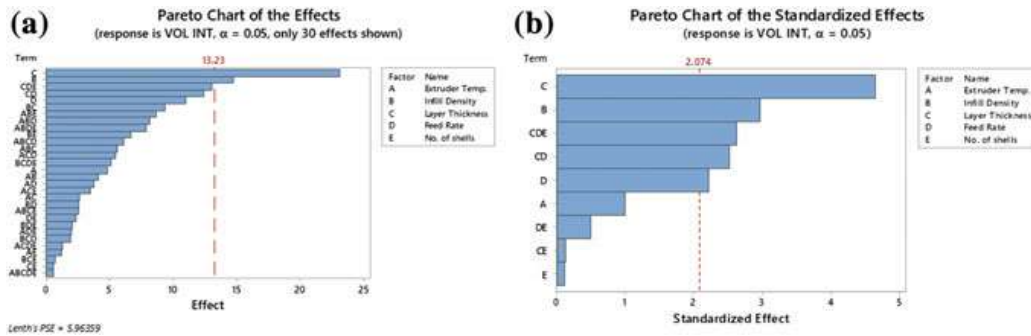


Fig. 18.10 Pareto chart of the factor effects of internal volume

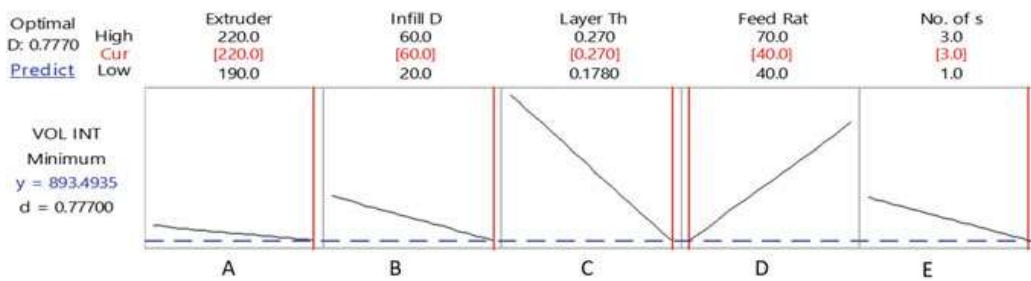


Fig. 18.11 Optimal values using optimizer Minitab tool for internal dimensions

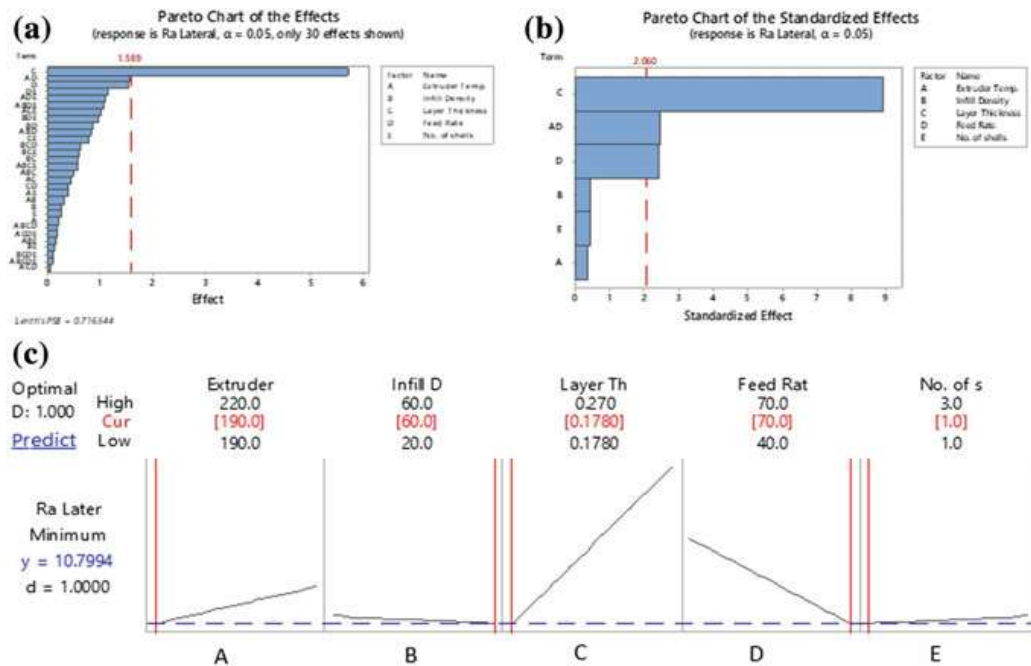


Fig. 18.12 Pareto charts and optimum levels for lateral surface roughness using Minitab optimizer

Table 18.4 Optimal factor values for volume and roughness

Factor	External volume	Internal volume	Ra lateral	Ra upper	Selected levels
Extruder temperature (°C)	190	220 ^a	190 ^a	190	190
Infill density (%)	20	60	60 ^a	60	60
Layer thickness (mm)	0.178	0.270	0.178	0.178	0.178
Print speed (mm/s)	40	40	70	40	40
No. of shells	3	3	1 ^a	3	3

^aNonsignificant

(AD) have a significant effect over the lateral surface roughness. According to Fig. 18.12b, significant and nonsignificant terms affect the lateral surface roughness response.

Layer thickness, extruder temperature, and print speed are the factors that should be controlled while the infill density and number of shells do not have a significant impact on lateral roughness response, as it can be seen in Fig. 18.12c where there is no significant difference between low and high level for the factors B and E. Table 18.4 shows recommended settings for optimal values to minimize lateral surface roughness.

18.3.4 Upper Surface Roughness Response Analysis

Figure 18.13a shows the results of the upper surface roughness analysis. Figure 18.13b shows results without nonsignificant effects for upper surface roughness test. Four main effects (A, C, D, and E), five two-term interactions (CD, AC, BC, AD, and BD), and two three terms interactions (BCD and CDE) have a significant effect over the response. Figure 18.13c shows the results obtained to optimize upper surface roughness. Since all factors appear at least one time on the interactions, all of them should be controlled according to the optimizer results. Table 18.4 shows the settings of each factor to optimize the desired response, numbers marked with an asterisk corresponds to nonsignificant factors adjusted to low or high levels without any effect on the response.

18.3.5 Dimensional Analysis

We measured all samples to analyze the dimensional and geometric accuracy of the printed pieces. We found an important dimensional variation in relation to drawing specifications that could affect the part functionality. Table 18.5 shows the

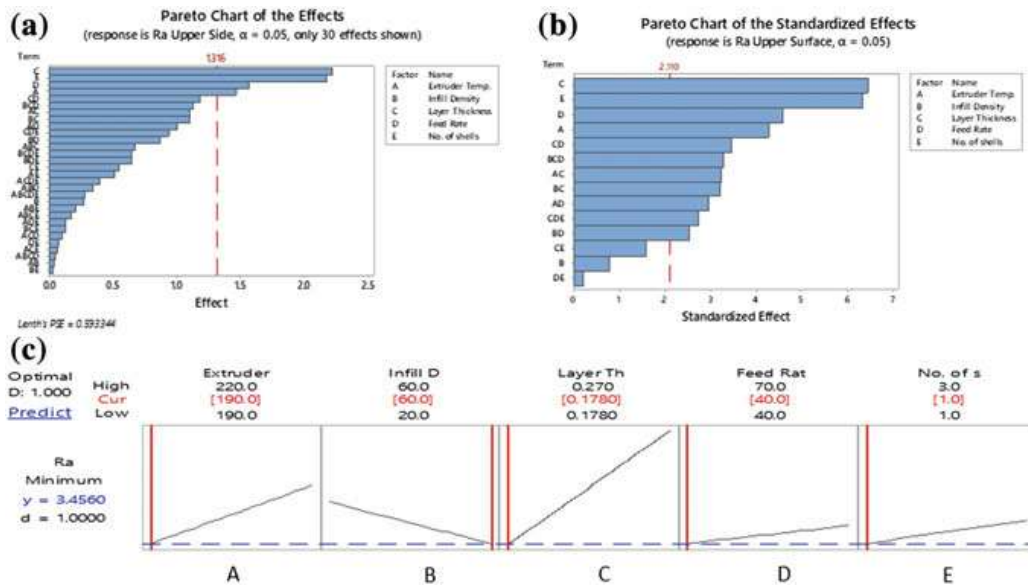


Fig. 18.13 Optimum levels for upper surface roughness using Minitab optimizer

dimensional results measured on the profile projector using DOE printer settings (columns 3–7), and Flashforge Creator Pro settings (columns 8–12). The first column shows the dimension label according to the drawing, the next column shows the dimension expressed in mm (reference value), the third column gives the average of all measurements, and the fourth column shows the average bias, while the fifth and sixth columns include the upper and lower limits of the acceptance criteria, and the seventh column is the decision-maker. Table 18.5 shows the same information for Flashforge settings on the last five columns.

Table 18.6 shows the variation expressed in the average percentage of measures for each dimension, and the significant deviations between the ideal dimension and the real one, on DOE and Flashforge Creator Pro settings. Most dimensions are below the drawing specifications, due mainly to PLA material properties that shrink during the cooling process from filament fusion temperature (180–220 °C) to room temperature. The effect of drastic temperature changes during the printing process could be reduced by heating the building print bed; however, this affects only the first layers of the printed piece.

18.3.6 Geometrical Analysis

Table 18.7 shows the results obtained from the measurements of the geometric dimensions of the model. The first column shows the feature shape, next column identifies the measurements used to calculate deviation in relation to the center point of the feature, third to sixth columns show to the measurements of the printed pieces under DOE adjustments, and the last four columns refer to the manufacturer recommended settings.

Table 18.5 Results of dimensional analysis

Dim.	Ref. value (mm)	DOE settings				Flashforge settings				Bias is accepted
		Ave. reading (mm)	Ave. bias (mm)	Lower limit (mm)	Upper limit (mm)	Ave. reading (mm)	Ave. bias (mm)	Lower limit (mm)	Upper limit (mm)	
1	17.50	17.523	0.0235	0.0006	0.040	17.569	0.069	0.034	0.104	NO
2	8.00	8.087	0.087	0.027	0.146	8.064	0.064	0.037	0.090	NO
3	4.00	3.869	-0.267	0.130	-0.059	3.843	-0.156	-0.191	-0.121	NO
4	4.00	3.826	-0.173	-0.199	-0.147	3.884	-0.116	-0.166	-0.065	NO
5	11.50	11.752	0.252	0.213	0.290	11.643	0.143	0.105	0.182	NO
6	16.50	16.465	-0.034	-0.074	-0.005	16.362	-0.137	-0.166	-0.109	NO
7	5.00	4.975	-0.025	-0.046	-0.003	4.945	-0.055	-0.079	-0.030	NO
8	10.00	10.092	0.092	0.072	0.111	10.034	0.034	-0.001	0.068	YES
9	21.00	21.015	0.015	-0.028	0.058	21.031	0.031	0.128	0.050	NO
10	8.00	7.644	-0.356	-0.385	-0.326	7.671	-0.328	-0.375	-0.281	NO
11	27.00	26.948	-0.051	-0.076	-0.026	26.945	-0.055	-0.087	-0.022	NO
12	21.00	20.987	-0.013	-0.058	0.032	21.058	0.058	0.028	0.087	NO
13	8.00	7.675	-0.324	-0.348	-0.300	7.759	-0.240	-0.264	-0.216	NO
14	8.00	7.623	-0.377	-0.399	-0.354	7.704	-0.296	-0.329	-0.262	NO
15	35.00	35.094	0.094	0.055	0.132	35.112	0.112	0.077	0.147	NO
16	8.00	8.203	0.203	0.040	0.365	8.352	0.352	0.124	0.579	NO
17	29.00	29.140	0.140	0.093	0.187	28.635	-0.346	-1.446	0.753	YES
18	5.66	6.008	0.348	0.288	0.407	5.777	0.117	0.048	0.185	NO
19	45.00 ^o	45.269 ^o	0.269	-0.130	0.551	45.743 ^o	0.743	0.447	1.038	NO
20	10	9.921	-0.078	-0.104	-0.052	9.901	-0.099	-0.141	-0.056	NO

Table 18.6 Percentage of variation in relation to reference value

Dim.	Ref value (mm)	Variation DOE settings (%)	Variation Flashforge settings (%)	Dim.	Ref value (mm)	Variation DOE settings (%)	Variation Flashforge settings (%)
1	17.50	0.13	0.40	11	27.00	-0.19	-0.20
2	8.00	1.09	0.80	12	21.00	-0.06	-0.28
3	4.00	-6.68	-3.90	13	8.00	-4.05	-3.00
4	4.00	-4.33	-2.90	14	8.00	-4.71	-3.70
5	11.50	2.19	1.24	15	35.00	0.27	0.32
6	16.50	-0.21	-0.83	16	8.00	2.54	4.40
7	5.00	-0.50	-1.10	17	29.00	0.48	-1.19
8	10.00	0.92	0.34	18	5.66	6.15	2.07
9	21.00	0.07	0.15	19	45.00 ^O	0.60	1.65
10	8.00	-4.45	-4.10	20	10	-0.78	-0.99





Third and seventh columns show the average actual position expressed in mm. In this table, we can observe a greater deviation on the internal features compared to the external feature identified by (5, 6) position deviation is only 0.02 mm compared with internal features where deviation exceeds the 0.2 mm. Columns four and five show the bias upper and lower limits. Column six shows the decisions for the DOE settings, while Flashforge settings are shown in the last three columns.

18.4 Conclusions

We concluded that the MSA bias concept could be used as an alternative, and an easy to use, method to evaluate the accuracy of commercial 3D printers that use fused filament deposition technique in order to determine the dimensional and geometric performance of the printer with specific materials, since this information is not given by the manufacturer in most cases.

We did not find a significant difference between the DOE optimal settings printer adjustments and manufacturer recommended settings for dimensional and geometrical analysis. Bias acceptance criteria for dimensional analysis rejected most of the evaluated dimensions. However, 4 out of 20 parts printed using DOE settings meet the acceptance criteria while only two dimensions of printed pieces using manufacturer recommended setup meet the acceptance bias criteria. We found comparing the average bias for each setup that about half of the dimensions of the DOE setup are smaller than the manufacturer recommended setup. The same situation is present in the geometric analysis, where only one out of four features evaluated meets the bias acceptance criteria using manufacturer recommended setup and none using DOE parameters setup, the average bias presents same behavior

Table 18.7 Geometrical analysis

Feature	Dim. (x_1, y_1)	DOE settings				Flashforge settings			
		$\bar{\phi}$ Average (mm)	Lower limit (mm)	Upper limit (mm)	Bias is accepted	$\bar{\phi}$ Average (mm)	Lower limit (mm)	Upper limit (mm)	Bias is accepted
	(1, 2)	0.244	0.162	0.328	NO	0.230	0.178	0.282	NO
	(5, 6)	-0.108	-0.143	-0.073	NO	0.003	-0.028	0.022	SI
	(8, 9)	0.248	0.156	0.191	NO	0.167	0.126	0.208	NO
	(11, 12)	0.310	0.217	0.306	NO	0.215	0.167	0.263	NO

than the dimensional analysis, so the conclusion is that there is no difference between the DOE and the manufacturer recommended setup.

3D printers are able to process different types of materials and produce at low cost with enough quality for prototyping parts; 3D printers have become a useful tool for companies that have capabilities to handle this technology since it facilitates and encourages innovation. For this reason, there is a high interest of companies to evaluate the accuracy of low-cost 3D printers in order to improve their processes.

Surface roughness depends on the print direction of the parts; therefore, it is important which side of the part is the upper face and which are the lateral sides. For lateral roughness, layer thickness, extruder temperature, and print speed are the factors that should be controlled while infill density and number of shells are nonsignificant factors. Nevertheless, all five factors evaluated in DOE should be controlled to get the optimal roughness on the upper surface of the printed piece.

Further analysis is required to determine causes of variation, in order to take actions to correct them and improve the quality of printed parts. The α level can also be modified but it depends on the level of sensitivity associated with the loss of function of the printed part. One source of variation is the drastic temperature change during the print process when the material (PLA) changes from fused to room temperature, the cooling process shrinking causes this variation. However, dimensional variation does not follow a consistent pattern, and percentage of variation in some dimensions could be too high for some applications where a dimensional performance is important for the part functionality.

We recommend performing studies with different filament materials in order to find which filament material gives a better dimensional performance, based on the different thermal properties.

References

- Automotive Industry Action Group (2010) MSA-4 Measurement systems analysis. <http://www.aiag.org/store/publications/details?ProductCode=MSA-4>
- Cajal C, Santoralia J, Velazquez J, Aguado S, Abajez J (2013) Volumetric error compensation technique for 3D printers. *Proc Eng* 63:126–132. <https://www.sciencedirect.com/science/article/pii/S1877705813014896>
- Campbell T, Williams C, Ivanova O, Garrett B (2011) Could 3D printing change the world?. Atlantic council, strategic foresight report, Oct 2011, pp 1–14
- Dassault Systems (2016) SolidWorks corporation. Available at: <http://Solidworks.es/sw> date accessed: 14 06 2016
- Dawoud M, Taha I, Ebeid S (2016) Mechanical behaviour of ABS: an experimental study using FDM and injection moulding techniques. *J Manuf Process* 21:39–45. <https://www.sciencedirect.com/science/article/pii/S1526612515001395>
- Evans B (2012) *Technology in action practical 3D printers: the science and art of 3D printing*. Apress Media, New York, USA
- FlashforgeUSA (2017) FlashforgeUSA. Available at: <http://www.flashforge-usa.com> date accessed: 16 05 2017

- Galantucci L, Bodi I, Kacani J, Lavecchia F (2015) Analysis of dimensional performance for a 3D open source printer based on fused deposition modeling technique. *Proc CIRP* 28:82–87. <https://doi.org/10.1016/j.procir.2015.04.014>
- Gebler M, Schoot-Uiterkamp A, Visser C (2014) A global sustainability perspective on 3D printing technologies. *Energy Policies* 74:215–243. <https://doi.org/10.1016/j.enpol.2014.08.033>
- Hoeken Z, Kintel M, Mayer A, Mets M (2012) ReplicatorG. Lowering the barrier to 3D printing at <http://replicat.org> date accessed: 18 04 2017
- ISO 1101 (2012) Geometrical product specifications (GPS)—geometrical tolerancing—tolerances of form, orientation, location and run-out. Available at: <https://www.iso.org/obp/ui/es/#iso:std:iso:1101:ed-4:v1:en> date accessed: 19 06 2017
- ISO4287 (1997) Geometrical product specifications (GPS)—Surface texture: profile method—terms, definitions and surface texture parameters. Available at: <https://www.iso.org/standard/10132.html> date accessed: 18 04 2017. (in Switzerland)
- Montgomery DC (2001) *Design and analysis of experiments*. Wiley, New York
- Nunez P, Rivas A, Garcia EBE, Sanz A (2015) Dimensional and surface texture characterization in fused deposition modelling (FDM) with ABS plus. *Proc Eng* 132:856–863. <https://doi.org/10.1016/j.proeng.2015.12.570>
- Rayna T, Striukova L (2016) From rapid prototyping to home fabrication: how 3D printing is changing business model innovation. *Technol Forecast Soc Change* 102:214–224. <https://doi.org/10.1016/j.techfore.2015.07.023>
- Roberson D, Espalin D, Wicker R (2013) 3D printer selection: a decision-making evaluation and ranking model. *Virtual Phys Prototyping* 8(3):201–212. <https://doi.org/10.1080/17452759.2013.830939>
- Satyanarayana B, Jaya K (2015) Component replication using 3D Printing technology. *Proc Mater Sci* 10:263–269. <https://doi.org/10.1016/j.mspro.2015.06.049>
- Stahl JE, Schultheiss F, Hagglund S (2011) Analytical and experimental determination of the Ra surface roughness during turning. *Proc Eng* 19:349–356. <https://doi.org/10.1016/j.proeng.2011.11.124>
- Stanbury JIM (2016) 3D printing with polymers: challenges among expanding options and opportunities. *Dent Mater* 32:54–64. <https://doi.org/10.1016/j.dental.2015.09.018>
- Walpole R, Myers R, Myers S (1999) *Probability and statistics for engineers*. Prentice Hall Hispanoamericana S.A. Mexico (in Spanish)
- Warren J, Duff J (1994) *Fundamentals of drawing in engineering*. Prentice Hall Inc, Mexico (in Spanish)